Journal of
Materials Chemistry B

PAPER

View Article Online
View Journal | View Issue

Cite this: J. Mater. Chem. B, 2016, 4, 5144

Sequential and controlled release of small molecules from poly(*N*-isopropylacrylamide) microgel-based reservoir devices†

Yongfeng Gao, Ka Yee Wong, Andrews Ahiabu and Michael J. Serpe*

Received 8th April 2016,
Accepted 8th July 2016

DOI: 10.1039/c6tb00864j

www.rsc.org/MaterialsB

Systems composed of a poly(*N*-isopropylacrylamide)-*co*-acrylic acid (pNIPAm-*co*-AAc) microgels (AAc-MG) and poly(*N*-isopropylacrylamide-3-(acrylamido)phenylboronic acid) (pNIPAm-*co*-APBA) microgels (APBA-MG) were used to sequentially release small molecules to a system in a controlled and triggered fashion. Specifically, at pH 10.0, methylene blue (MB, positively charged) exhibited strong electrostatic interactions with both the negatively charged AAc and APBA-modified microgels. This resulted in MB uptake into both of the microgels. At pH 7.0, the APBA groups were neutralized, allowing MB to be released from the APBA-MG only. When the solution pH was again lowered to 3.0, the AAc groups are neutralized allowing MB to be released from the AAc-MG. By incorporating the mixed microgels into reservoir devices, and varying their ratio, the small molecule release rate and release amount (dosage) can be easily tuned. Furthermore, two different small molecules can be loaded into the two distinct microgels, which allows for their sequential release at particular pHs. These devices could find use for delivering multiple drugs to a system in a controlled and triggered fashion, which may find a variety of biomedical applications.

Introduction

Controlled and triggered drug delivery systems have played a major role in improved disease treatment over the past few decades.[1–6] This is in part due to their ability to render otherwise toxic drug treatments relatively non-toxic by controlling dosages through controlled release rates. Most materials to date have been engineered to deliver a single small molecule drug to a system, and many are commercially available, such as the Cypher® stent from Johnson & Johnson, and the Taxus® stent from Boston Scientific. These, and similar devices, can be generated by mixing drug molecules with degradable polymers, which degrade under certain conditions to release a small molecule at a given rate. While these materials have certainly enhanced human health, many medical conditions are controlled by multiple biomolecules. Therefore, comprehensive treatment of certain diseases and conditions may be more effectively achieved by delivering more than one drug at a time to a system. Recently, the concept of multi-drug therapy was introduced[7–10] and systems that deliver multiple small molecules at the same time (co-delivery)[11] or sequentially[12] have been developed. For example, CombiPatch®, a transdermal patch marketed by Novogyne Pharmaceuticals, is a drug delivery system that can release both estradiol (an estrogen) and norethindrone acetate (a progestin) continuously upon application to the skin and delivers the medication in a steady and predictable manner for hormone replacement therapy. Similar approaches to drug delivery may provide great improvements to achieve enhanced therapies.

To yield enhanced delivery systems, various materials have been utilized, such as inorganic nanomaterials,[13] polymers,[2,14–16] and biomacromolecules.[17–19] Among these, polymers have played an integral role in advanced drug delivery technologies, allowing both hydrophilic and hydrophobic drugs to be released at constant (or variable) rates over long periods of time. One approach utilized small molecule ''drug'' loaded polymer-based ''reservoirs'', which allowed for diffusion-controlled drug release.[3,20] Another approach relied on covalently[21,22] or non-covalently bonding[23] drug molecules onto/into a carrier; the bond between the drug and the carrier can be broken at certain environmental conditions,[24] *e.g.*, in the presence of an enzyme,[25] and/or at certain pH values.[26]

Responsive polymers have also found their way into many drug delivery systems, with poly(*N*-isopropylacrylamide) (pNIPAm) being the most utilized to date.[27–30] PNIPAm is well known to be thermo-responsive, exhibiting a lower critical solution temperature (LCST) at 32 °C in water. That is, at temperature (T) < 32 °C

Department of Chemistry, University of Alberta, Edmonton, Alberta, Canada T6G 2G2. E-mail: michael.serpe@ualberta.ca

† Electronic supplementary information (ESI) available: MB UV-vis spectrum; images of samples before and after MB loading. See DOI: 10.1039/c6tb00864j

the polymer has favorable interactions with water molecules and exists as a solvated, extended random coil. The polymer–polymer interactions become dominant at $T > 32$ °C, causing the polymer to desolvate and collapse into a dense globular conformation.[31,32] Furthermore, the transition is fully reversible and can be repeated many times. As the LCST is close to physiological temperature, pNIPAm-based materials, such as hydrogels and microgels have been widely exploited extensively for biomedical and biological applications. Like linear pNIPAm, pNIPAm-based hydrogel particles (microgels) have also been synthesized and are fully water swollen (large diameter) at $T < 32$ °C, while they are dehydrated (small diameter) at $T > 32$ °C. PNIPAm-based micro and nanogels are most easily synthesized *via* free radical precipitation polymerization.[33–36] This approach is versatile in terms of the variety of chemical functionality that can be added to the microgels by simply adding functional monomers to the reaction prior to the initiation. Using this approach, pNIPAm-based microgels with a variety of chemical functionalities have been synthesized. The most commonly used comonomer is acrylic acid (AAc), which renders pNIPAm-*co*-AAc microgel pH responsive;[37–39] AAc can also be used to couple other small molecules to the microgels by various coupling chemistries. The pH responsivity of the pNIPAm-*co*-AAc microgels is a direct result of the weak acidity of the AAc group. AAc has a pK_a of ~4.25, therefore when the pH of their environment is <4.25, the AAc groups are protonated and mostly neutral (a slight charge can exists depending on the initiator used), while they are negatively charged when at pH > 4.25. As a result, at high pH, the microgels have attractive electrostatic interactions with positively charged species, while at low pH they have minimal interactions with positively charged species. Similarly, other weak acid/base modified microgels can be synthesized, *e.g.*, in this submission we generated boronic acid modified microgels by copolymerization of 3-(acrylamido)phenylboronic acid (APBA) into the microgels.[29,40–42] APBA exhibits a pK_a of ~8.4 and is therefore negatively charged at pH > 8.4, while APBA is neutral at pH < 8.4. Like AAc-modified microgels, the APBA-modified microgels exhibit attractive interactions with positively charged species at high pH, while they are neutralized, and have minimal interactions with positively charged species at lower pH (<8.4).

PNIPAm has found its way into controlled/triggered drug delivery devices mainly due to its above-described thermoresponsivity, which occurs close to body temperature[24,43–45] Recently, our group developed a pNIPAm microgel-based optical device (etalon) that we demonstrated to be very useful for sensing and biosensing.[37,46–51] The structure of the etalon can be seen in Fig. 1. We also showed that this device structure could be used as a "reservoir" for small molecules, allowing controlled and triggered release of the small molecules to a system.[52–54] Specifically, by localizing a small molecule into the microgel layer, we showed that the thickness of the Au layer covering the microgels (overlayer) allowed control over release rates; this due to the tunability of the Au pore size with its thickness.[46,53] That is, thick Au has fewer and smaller pores than thin Au, which allows small molecules to exit the microgel layer either slow or fast, respectively.[53]

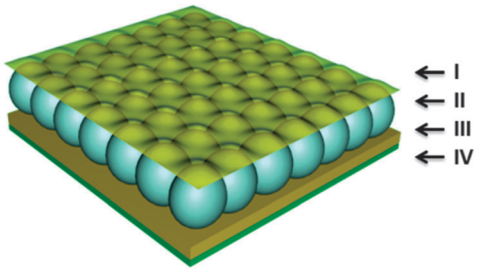

Fig. 1 The structure of a standard microgel-based etalon composed of two Au layers (I and III) sandwiching a microgel layer (II), all on a glass support (IV).

In the present work, we combined the ability to control the release rate of small molecules from our reservoir devices with the ability to tailor microgel chemistry to produce a system capable of delivering small molecules only at a specific solution pH and at controlled rates. This was accomplished by constructing reservoir devices from pNIPAm-*co*-AAc and pNIPAm-*co*-APBA microgels, which respond to pH by ionizing over drastically different ranges; the ionization (and neutralization) is what allows small molecules to be released only at drastically different solution pHs. We believe that these systems can provide more options for sequential and controlled drug release or multi-drug delivery approaches to therapy.

Results and discussion

A schematic of the drug loading mechanism is shown in Fig. 2. The model drug used in this study was methylene blue (MB). As the structure shows, MB is a positively charged molecule, which can interact strongly with negative charged moieties. In this study, two sets of microgels were synthesized, pNIPAm-*co*-AAc (AAc-MG) and pNIPAm-*co*-APBA (APBA-MG), which are both pH responsive. Specifically, these groups are negatively charged at pH > 4.25 and 8.4, respectively, but are neutral at pHs below these respective pH values. The microgels were loaded with MB by exposing them to solutions at pH 10.0, which was high enough to render both sets of microgels negatively charged, while the MB remained positively charged. This allowed the MB to be absorbed by the microgels *via* electrostatic interactions, as

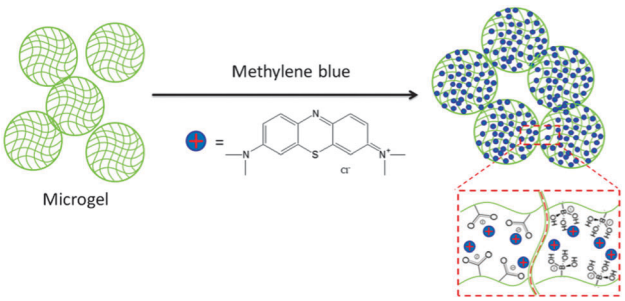

Fig. 2 Positively charged methylene blue was used as a model drug molecule that can be loaded into AAc-MG and APBA-MG at solution pH that renders them negatively charged.

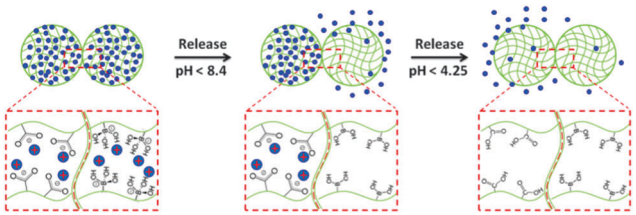

Fig. 3 Schematic of the pH triggered MB release from APBA-MG and AAc-MG. As each microgel is neutralized, the electrostatic interactions between the microgel and the MB are diminished, and the MB is released from the microgel.

shown schematically in Fig. 2. After loading, and washing away the excess MB with pH 10.0 solution, the microgels exhibited a blue color; this confirmed that the MB was loaded into the microgel.

After MB was loaded into the microgels, we investigated their ability to release MB in a pH-triggered fashion. Specifically, when the solution pH is >8.4, both the APBA-MG and AAc-MG will be negatively charged, and will bind the MB strongly. When the solution pH is decreased below the pK_a for APBA, MB will be released from APBA-MG, while MB will still be bound to the AAc-MG. MB will then be released from the AAc-MG when the solution pH is below the AAc pK_a. The hypothesized release mechanism is shown schematically in Fig. 3.

To test this hypothesis, we first investigated the pH-dependent release properties for the microgels in solution. To accomplish this, we first mixed 250 μL of AAc-MG, 250 μL of APBA-MG, and 200 μL MB (0.5 mg mL^{-1}) and diluted into 10.0 mL pH 10.0 solution. This mixture was incubated for 3 h to load the MB into the microgels. The unbound MB was removed from the MB loaded microgels by multiple centrifugation/resuspension cycles, as detailed in the Experimental section. Then, 25 μL of the mixed concentrated microgel solution was exposed to various pH solutions to characterize their release behavior. Specifically, the microgels were incubated at each specific pH for 3 h (sufficient time for MB to diffuse out of microgels), then the microgels were centrifuged and the UV-vis spectrum of the supernatant solution was acquired. The absorbance value at 664 nm (λ_{max} for MB, the full spectrum can be seen in electronic supporting information (ESI,† Fig. S1)) was then plotted as a function of solution pH. As can be seen in Fig. 4, when the solution pH was 10.0, only a small amount of MB was released from the microgels. At pH 9.0 to 7.0, there was a dramatic release of MB due to the neutralization of the APBA groups. At pH 7.0 to 5.0, there was minimal MB release, while another dramatic release event was observed when the solution pH was decreased to 4.0, which corresponds with the AAc–MB interaction weakening due to AAc neutralization. Finally, at pH 4.0 to 2.0, all the MB was released, and the solution concentration of MB was stable. This result shows that sequential delivery of a small molecule from microgels is possible.

Next, we wanted to demonstrate that the release rate of the MB could be controlled using microgel-based reservoir devices. The devices were constructed by "painting" the mixed microgels (mixed at a ratio of 1 : 1 (v/v) prior to painting) onto a

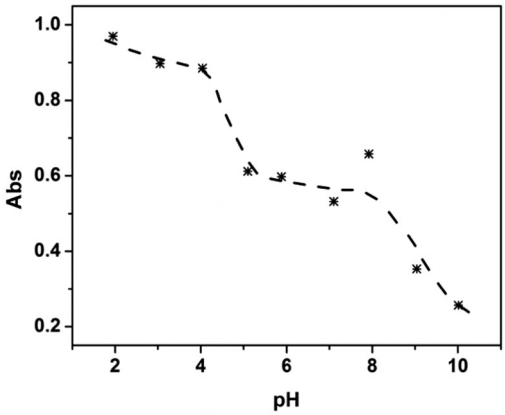

Fig. 4 The maximum absorbance at 664 nm (λ_{max} for MB) obtained from a UV-vis of the supernatant solutions at each of the indicated solution pHs. In this case, the microgels were dispersed in solution at the indicated pH.

Au-coated glass slide, following previously published protocols.[55] Again, the device structure is shown in Fig. 1. It is important to note that the microgels were first painted on the Au-coated glass slide, then loaded with MB by soaking in a MB solution at pH 10.0. Photographs of the MB loaded slides can be seen in ESI,† Fig. S2. Following MB loading, 50 nm of Au was deposited on the top of the microgel layer *via* thermal evaporation. Finally, the edges were sealed with clear nail polish to prevent MB release from the sides of the device.[53] The devices were soaked in a pH 10.0 solution, and the solution pH was systematically decreased. The release profiles for the devices at 37 °C and 25 °C are shown in Fig. 5. As can be seen in Fig. 5a (37 °C), the signal was stable until the solution pH was adjusted to 7.0 by addition of 0.1 M HCl. At this pH the APBA microgels were neutralized, which caused them to release their loaded MB. After ~14 min, the solution absorbance stabilized, and then the solution pH was further decreased to 3.0. At this point we observed another dramatic increase in MB concentration in solution due to the AAc neutralization and their release of MB. After some time (~25 min), the MB concentration in solution was stable due to the device being completely depleted of MB to release. The release behavior at 25 °C is shown in Fig. 5b, and as can be seen,

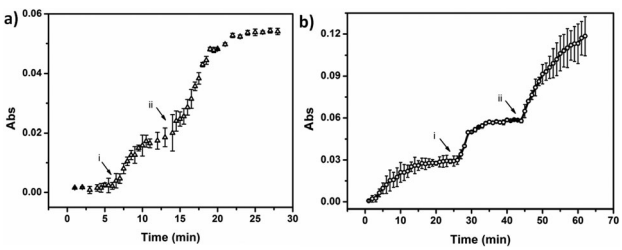

Fig. 5 The maximum absorbance at 664 nm (λ_{max} for MB) obtained from a UV-vis of the solution in a Petri dish containing a reservoir device with 1 : 1 APBA-MG and AAc-MG and 50 nm Au overlayer at (a) 37 °C and (b) 25 °C. The solution pH was changed from 10.0 to (arrow i) 7.0 and (arrow ii) 3.0. Each data point is an average value obtained from the analysis of two separate reservoir devices, with the error bars indicating the standard deviation.

the release behavior is similar to what was observed at 37 °C. Upon close inspection, it appears that the release kinetics at both temperatures were approximately the same when the solution pH was decreased from pH 10.0 to 7.0. Although, the device at 37 °C appeared to release faster than the device at 25 °C when the solution pH was further decreased from 7.0 to 3.0. This observation could be the result of many different factors (*e.g.*, slightly different LCSTs for the microgels, and/or different total microgel diameter changes for the microgels after collapse), which need to be investigated more carefully. This will be investigated further, but we feel that those experiments are out of the scope of the present submission.

For comparison, we investigated the pH dependent MB release profile for the mixed microgels (1 : 1 (v/v)) in solution. This was done by mixing 200 μL of each of the drug-loaded microgels into 10.0 mL pH 10.0 solution in a centrifuge tube. After soaking for 3 h, the whole sample was centrifuged to cause the microgels to be forced to the bottom of the centrifuge tube, and 1 mL of the supernatant solution was analyzed *via* UV-vis spectroscopy. The supernatant solution was returned to the original centrifuge tube and the solution was mixed and left to incubate for more time. At certain points, the solution pH was changed to pH 7.0 and 3.0, and the data can be seen in ESI,† Fig. S3. Compared to the microgel-based reservoir device, the free microgels release much more slowly, and take much longer to completely release the MB. Specifically, the release triggered from the first step takes ~4 h to stabilize, but the second pH-triggered release continues for days.

To further prove that the release rate from the reservoir devices can be tuned by varying the thickness of the reservoir device's Au overlayer, we prepared samples with two different Au overlayer thicknesses, 50 nm and 230 nm. To make the devices here, the painting procedure was varied slightly compared to what is described above. Specifically, to achieve the desired 1 : 1 ratio of APBA-MG : AAc-MG, half of each substrate was painted with APBA-MG, and the other half was painted with AAc-MG. This was done to offer more control over the microgel ratios in the reservoir devices. That is, the nature of the painting procedure produces "monolithic" monolayers of microgels on the Au coated surfaces. This ensures that each half of the surface is completely covered with a similar amount of the respective polymers. This is not something that can be said for painting the mixed microgel solutions. Regardless, the release profiles are shown in Fig. 6. As can be seen, the device composed of a thin Au layer releases MB significantly faster than the devices composed of a relatively thick Au layer. This is due to the smaller pores of the thick Au overlayers restricting access of the MB to the bulk solution; thin Au has many pores, which isn't as effective at restricting access of the MB to the solution as the thick Au.[48] We point out that the release profile for the devices made for this experiment is similar to what was observed in Fig. 5 (painting the mixed microgels), which proves that the painting protocol used to make these devices doesn't greatly alter the observed release behavior.

We point out that for all the experiments above, the ratio of APBA-MG : AAc-MG was 1 : 1. As can be seen from the data, the

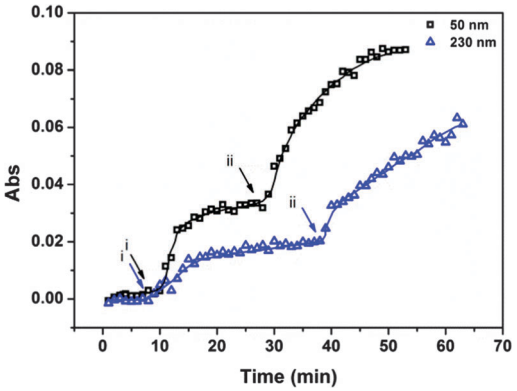

Fig. 6 The maximum absorbance at 664 nm (λ_{max} for MB) obtained from a UV-vis of the solution in a Petri dish containing a reservoir device with 1 : 1 APBA-MG and AAc-MG with a Au overlayer thickness of (□) 50 nm and (Δ) 230 nm. The solution pH was changed from 10.0 to (arrow i) 7.0 and (arrow ii) 3.0.

amount of MB released as a result of the solution pH changes is not the same when stepping from pH 10.0 to 7.0 and from pH 7.0 to 3.0. This suggests that the APBA-MG and AAc-MG have different capacities for releasing MB. This could be a result of the different microgel chemistries, which can influence their interactions with MB. This could also be a result of a mismatch in the number of each ionizable groups in the respective microgels of the reservoir devices. Understanding this behavior would require more experimentation, which will be the subject of another investigation. For this investigation, we wanted to show that we could control the amount of MB released at the different pHs. In that case, we prepared reservoir devices by painting surface with 4 : 1 APBA-MG : AAc-MG and 1 : 1 APBA-MG : AAc-MG. The microgels were loaded with MB, and we investigated the pH triggered release by UV-vis. The results can be seen in Fig. 7. As can be seen, when the ratio was 1 : 1, ~30% of the release was from the APBA-MG (the pH 10.0 to 7.0 change) and ~70% was from the AAc-MG (pH 7.0 to 3.0 change). However, when the ratio was 4 : 1, the release from each of the microgels was approximately equal. This represents a very powerful yet simple

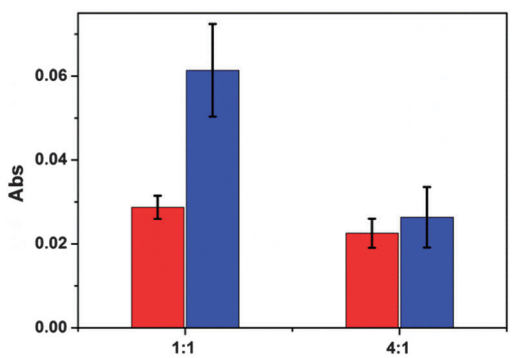

Fig. 7 The absorbance values for the two separate pH triggered releases observed for reservoir devices containing 1 : 1 and 4 : 1 APBA-MG : AAc-MG. The red bars are for the APBA-MG and the blue bars are for the AAc-MG. The values are an average of two separate measurements, and the error bars indicate the standard deviation.

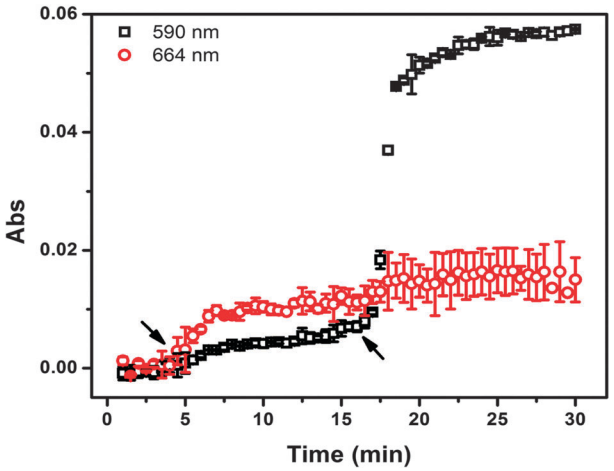

Fig. 8 The release profile for a device made of APBA-MG and AAc-MG loaded with MB and CV, respectively. The arrow at ~4 min shows the time the solution pH was adjusted to 7.0, while the arrow at ~17 min indicates when the solution pH was decreased to 3.0. The data points are averages obtained from two seperate devices, and the error bars indicate the standard deviation.

approach to precisely control the amount of small molecules delivered to a system. For example, an array of reservoir devices can be fabricated on a single substrate, each containing different ratios of microgels, which will allow one to rationally design the specific release characteristics. Furthermore, this can be combined with the tunable release kinetics (by changing the Au overlayer thickness) to provide even more control over small molecule doses.

Finally, we determined the ability of the devices to release more than one small molecule when triggered by pH. For these experiments, MB and crystal violet (CV),[52,53] were used, and were separately loaded into APBA-MGs and AAc-MGs. The release profile from these devices can be seen in Fig. 8. As can be seen, when the solution pH was decreased to 7.0 at ~4 min, MB that was loaded in the APBA-MG was released. However, the CV in AAc-MG was not released until the solution pH was adjusted to 3.0. We point out that there was some overlap in the absorbance spectra for MB and CV, and therefore there was an increase in the CV signal (590 nm) when the MB was triggered to release, and *vice versa*. While this is the case, there may be some MB and CV released nonspecifically from the respective microgels. Regardless, the results suggest that the devices could be used to sequentially release small molecules to a system in a pH dependent fashion.

Experimental

Materials

N-Isopropylacrylamide (NIPAm) was purchased from TCI (Portland, Oregon) and purified by recrystallization from hexanes (ACS reagent grade, EMD, Gibbstown, NJ) prior to use. *N*,*N*′-Methylenebisacrylamide (BIS) (99%), acrylic acid (AAc) (99%), 3-(acrylamido)phenylboronic acid (APBA) and ammonium persulfate (APS) (98+%) were obtained from Aldrich (St. Louis, MO) and were used as received. Sodium chloride was obtained from EMD (Millipore, Billerica, MA), and deionized (DI) water with a resistivity of 18.2 MΩ cm was used. Cr/Au annealing was done in a Thermolyne muffle furnace from ThermoFisher Scientific (Ottawa, Ontario). Anhydrous ethanol was obtained from Commercial Alcohols (Brampton, Ontario). Sodium hydroxide (NaOH, 99.8%) and hydrochloric acid were purchased from Caledon Chemicals (Georgetown, Ontario) and were used as received. Fisher's finest glass coverslips were 25 × 25 mm and obtained from Fisher Scientific (Ottawa, Ontario). Cr was 99.999% and obtained from ESPI as flakes (Ashland, OR), while Au was 99.99% and obtained from MRCS Canada (Edmonton, AB). Methylene blue (MB) and crystal violet (CV) was obtained from Sigma-Aldrich.

Microgel synthesis

Microgels composed of poly(*N*-isopropylacrylamide)-*co*-acrylic acid (pNIPAm-*co*-AAc) were synthesized *via* free radical precipitation polymerization as described previously.[48] Briefly, a 3-necked round bottom flask was fitted with a reflux condenser, nitrogen inlet, and temperature probe, and charged with a solution of NIPAm (11.9 mmol) and BIS (0.703 mmol) in 99 mL deionized water, previously filtered through a 0.2 μm filter. The solution was bubbled with N_2 gas and allowed to heat to 70 °C over ~1 hour. AAc (1.43 mmol) was added to the heated reaction mixture in one aliquot. The reaction was then initiated with a solution of APS (0.2 mmol) in 1 mL of deionized water. The reaction was allowed to proceed at 70 °C for 4 hours under a blanket of nitrogen. The resulting suspension was allowed to cool overnight, and then it was filtered through a Whatman #1 paper filter to remove any large aggregates. The microgel solution was then distributed into centrifuge tubes and purified *via* centrifugation at ~8300 rcf to form a pellet, followed by removal of the supernatant and resuspension with deionized water, 6×. The cleaned microgels were recombined and stored in a brown glass jar. Poly(*N*-isopropylacrlamide-3-(acrylamido)phenylboronic acid) (pNIPAm-*co*-APBA) microgels were synthesized in the same manner but replacing the AAc with APBA. The pH responsivity of the APBA-containing microgels is shown in ESI,† Fig. S4, while the pH responsivity for the AAc-containing microgels has been demonstrated previously.[52,53]

Loading MB into microgels

250 μL of highly concentrated pNIPAm-*co*-AAc microgels, 250 μL of highly concentrated pNIPAm-*co*-APBA microgels, and 200 μL of aqueous MB solution (0.5 mg mL^{-1}) was added into 10.0 mL pH 10.0 solution (in a centrifuge tube), vortexed for 30 s and soaked for 3 h. The solution was then centrifuged for 1 h at 10 000 rpm, the supernatant solution containing the unbound MB was removed, and the microgels resuspended at the bottom in pH 10.0 solution. This pH allowed the unbound MB to be separated from the MB loaded microgels. This process of centrifugation and resuspension was repeated 3 times.

MB release from mixed microgels in solution

25 μL of dye loaded mixed microgel solution was added to centrifuge tubes containing solutions with pH 2.0, 3.0, 4.0, 5.0,

6.0, 7.0, 8.0, 9.0, 10.0. The microgels were left exposed to these solutions for 3 h then centrifuged for 1 h at 10 000 rpm. We also prepared mixed microgel solutions to investigate the kinetics of MB release from the microgels in solution. This was done by mixing 200 μL of each drug-loaded microgels into 10.0 mL pH 10.0 solution, incubating for some time, then centrifuging to isolate the microgels from the supernatant solution. 1 mL of the supernatant solution was analyzed each time, which was completely returned back to the original solution in the centrifuge tube. The process was repeated many times, and the solution pH was varied by adding 1.0 M HCl. The absorbance value at 664 nm (λ_{max} for MB) was collected from a UV-vis spectrum obtained with an Agilent 8453 UV-vis spectrophotometer, equipped with an 89090A temperature controller and Peltier heating device.

Microgel-based reservoir device fabrication

2 nm Cr followed by 15 nm of Au was deposited *via* thermal evaporated (Torr International Inc., thermal evaporation system, Model THEUPG, New Windsor, NY) onto a 25 × 25 mm ethanol rinsed and N_2 gas dried glass coverslip (Fisher's Finest, Ottawa, ON) at a rate of 0.2 Å s^{-1}, and 0.1 Å s^{-1}, respectively. The Cr/Au substrates were annealed at 250 °C for 3 h (Thermolyne muffle furnace, Ottawa, ON) and cooled to room temperature prior to microgel film deposition. Approximately 10 mL of microgel solution was centrifuged at ~8300 rcf to form a pellet at the bottom of a centrifuge tube. The supernatant was removed and discarded, and the pellet was vortexed to loosen and homogenize the particles in the remaining solvent. A 40 μL aliquot of the concentrated microgels was added onto the substrate and then spread toward each edge using the side of a micropipette tip. The substrate was rotated 90°, and the microgel solution was spread again. The spreading and rotation continued until the microgel solution became too viscous to spread due to drying. The microgel solution was allowed to dry completely on the substrate for 2 h with the hot plate temperature set to 35 °C. The dry film was then rinsed copiously with DI water to remove any excess microgels not bound directly to the Au. The film was then placed into a DI water bath and allowed to incubate overnight on a hot plate set to ~30 °C. Following this step, the samples were then rinsed with deionized water, dried with N_2, and then immersed into a 20 mL solution of MB (0.5 mg mL^{-1}, pH of 10.0) overnight. Excess MB was rinsed off the substrate with pH 10.0 solution (to not disturb the microgel–MB interaction) and incubated in pH 10.0 solution overnight followed by drying with N_2 gas. Another Au overlayer (2 nm Cr and 50 nm Au) was evaporated onto the MB loaded microgel layer. Since we were interested in understanding how the Au overlayer affected the rate of MB release from the etalon, we sealed the etalon's edges with clear nail polish to ensure that the MB was being released through the Au overlayer. Previous studies have confirmed that this is effective at preventing small molecules from releasing from the sides of the reservoir devices.[48] To fabricate devices with different ratios of microgels, we followed the same procedure as above, with slight modification. Briefly, to generate the 4 : 1 samples, we coated 80% of the substrate with APBA-MG, and 20% with AAc-MG. For the 1 : 1 samples, half of the substrate was coated with APBA-MG and the other half coated with AAc-MG.

For loading MB and CV into APBA-MG and AAc-MG, respectively, we exposed the portion of the substrate coated with APBA-MG to the MB solution (0.5 mg mL^{-1}, pH 10.0) and the portion coated with AAc-MG to the CV solution (0.5 mg mL^{-1} in pH 7.0). After 3 h, the excess solutions were rinsed off the surfaces with pH 10.0 and pH 7.0 solutions, respectively. The microgels were then coated with a given thickness of Au and the edges sealed to prevent release from the side of the device.

Release from reservoir devices

A Petri dish containing 20 mL of pH 10.0 solution was placed on a hot plate, and the solution temperature maintained at either 37 °C or 25 °C. The solution in the Petri dish was stirred continuously at 260 RPM using a magnetic stir bar. The solution pH always began at 10.0, and was adjusted by addition of 0.1 M HCl. The solution flowed through a cuvette (*via* a peristaltic pump) in an Agilent 8453 UV-vis spectrophotometer, equipped with an 89090A temperature controller and Peltier heating device. MB loaded etalons were added to the Petri dish, and a timer started. The absorbance spectrum from the solution was collected every 60 s.

Conclusions

In summary, we showed that microgel-based reservoir devices could be fabricated from mixed microgels, specifically APBA-MG and AAc-MG. We went on to show that these microgels could load positively charged MB, which could be released sequentially to a system, in a pH dependent fashion. That is, when the solution pH was 10.0, both microgels were negatively charged and bound the MB strongly. When the solution pH was decreased to 7.0, the APBA-MG was neutralized and released MB; the AAc-MG was neutralized and released its MB when the pH was decreased to pH 3.0. The data obtained from the reservoir devices was compared to microgels in solution, which exhibited much slower release kinetics. We also showed that the release kinetics from the reservoir devices could be tuned by varying the Au overlayer thickness. Additionally, we showed that the amount of MB delivered to a system as a result of the pH changes could be tuned by changing the ratio of the APBA-MG and AAc-MG in the reservoir devices. Finally, we demonstrated that two different small molecules could be delivered to a system when triggered at specific pHs, *e.g.*, pH 7.0 and 3.0. These systems represent a versatile approach to sequentially delivering small molecules to a system, in a triggered fashion, with tunable release kinetics. Importantly, their release behavior can be easily tuned by simply changing the microgel chemistry, *e.g.*, by generating reservoir devices from microgels that ionize at different solution pH. This would allow one to deliver various small molecules to a system triggered by a variety of solution pHs. This, combined with the tunable release kinetics and the ability to array these devices on a single substrate, makes this delivery platform extremely versatile, powerful, and unique.

Acknowledgements

MJS acknowledges funding from the University of Alberta (the Department of Chemistry and the Faculty of Science), the Natural Sciences and Engineering Research Council of Canada (NSERC), the Canada Foundation for Innovation (CFI), the Alberta Advanced Education & Technology Small Equipment Grants Program (AET/SEGP), Grand Challenges Canada and IC-IMPACTS. YG acknowledges Alberta Innovates Technology Futures (AITF) for graduate student scholarships. KYW acknowledges financial support from the University of Alberta's Undergraduate Research Initiative.

Notes and references

1 R. Langer, *Nature*, 1998, **392**, 5–10.
2 K. E. Uhrich, S. M. Cannizzaro, R. S. Langer and K. M. Shakesheff, *Chem. Rev.*, 1999, **99**, 3181–3198.
3 R. Langer, *Science*, 1990, **249**, 1527–1533.
4 Y. Qiu and K. Park, *Adv. Drug Delivery Rev.*, 2012, **64**, 49–60.
5 B. Chertok, M. J. Webber, M. D. Succi and R. Langer, *Mol. Pharmaceutics*, 2013, **10**, 3531–3543.
6 S. J. Liu, S. Wen-Neng Ueng, S. S. Lin and E. C. Chan, *J. Biomed. Mater. Res.*, 2002, **63**, 807–813.
7 N. S. Rejinold, T. Baby, K. Chennazhi and R. Jayakumar, *J. Biomed. Nanotechnol.*, 2015, **11**, 392–402.
8 M. S. Aw, J. Addai-Mensah and D. Losic, *Chem. Commun.*, 2012, **48**, 3348–3350.
9 Q. He, Y. Gao, L. Zhang, Z. Zhang, F. Gao, X. Ji, Y. Li and J. Shi, *Biomaterials*, 2011, **32**, 7711–7720.
10 H.-C. Shin, A. W. Alani, D. A. Rao, N. C. Rockich and G. S. Kwon, *J. Controlled Release*, 2009, **140**, 294–300.
11 F.-M. Chen, M. Zhang and Z.-F. Wu, *Biomaterials*, 2010, **31**, 6279–6308.
12 A. C. Le Meur, C. Aymonier and V. Héroguez, *ChemPhysChem*, 2012, **13**, 692–694.
13 T. Sun, Y. S. Zhang, B. Pang, D. C. Hyun, M. Yang and Y. Xia, *Angew. Chem., Int. Ed.*, 2014, **53**, 12320–12364.
14 W. B. Liechty, D. R. Kryscio, B. V. Slaughter and N. A. Peppas, *Annu. Rev. Chem. Biomol. Eng.*, 2010, **1**, 149.
15 T. Vermonden, R. Censi and W. E. Hennink, *Chem. Rev.*, 2012, **112**, 2853–2888.
16 Y. Jiang, G. Liu, X. Wang, J. Hu, G. Zhang and S. Liu, *Macromolecules*, 2015, **48**, 764–774.
17 M. Malmsten, H. Bysell and P. Hansson, *Curr. Opin. Colloid Interface Sci.*, 2010, **15**, 435–444.
18 H. Zhang, M. Oh, C. Allen and E. Kumacheva, *Biomacromolecules*, 2004, **5**, 2461–2468.
19 X. Hu, G. Liu, Y. Li, X. Wang and S. Liu, *J. Am. Chem. Soc.*, 2014, **137**, 362–368.
20 P. J. Blackshear, *Sci. Am.*, 1979, **241**, 66.
21 J. Khandare and T. Minko, *Prog. Polym. Sci.*, 2006, **31**, 359–397.
22 J. Kopeček, *Adv. Drug Delivery Rev.*, 2013, **65**, 49–59.
23 J. Ding, L. Chen, C. Xiao, L. Chen, X. Zhuang and X. Chen, *Chem. Commun.*, 2014, **50**, 11274–11290.
24 S. Mura, J. Nicolas and P. Couvreur, *Nat. Mater.*, 2013, **12**, 991–1003.
25 M. R. Lee, K. H. Baek, H. J. Jin, Y. G. Jung and I. Shin, *Angew. Chem., Int. Ed.*, 2004, **43**, 1675–1678.
26 K. T. Oh, H. Yin, E. S. Lee and Y. H. Bae, *J. Mater. Chem.*, 2007, **17**, 3987–4001.
27 C. Wu and S. Zhou, *Macromolecules*, 1995, **28**, 8381–8387.
28 J. D. Debord and L. A. Lyon, *Langmuir*, 2003, **19**, 7662–7664.
29 T. Hoare and R. Pelton, *Macromolecules*, 2007, **40**, 670–678.
30 H. Kawaguchi, K. Fujimoto and Y. Mizuhara, *Colloid Polym. Sci.*, 1992, **270**, 53–57.
31 I. Berndt and W. Richtering, *Macromolecules*, 2003, **36**, 8780–8785.
32 R. Pelton, H. Pelton, A. Morphesis and R. Rowell, *Langmuir*, 1989, **5**, 816–818.
33 R. Pelton and P. Chibante, *Colloids Surf.*, 1986, **20**, 247–256.
34 J. Wiedemair, M. J. Serpe, J. Kim, J.-F. Masson, L. A. Lyon, B. Mizaikoff and C. Kranz, *Langmuir*, 2007, **23**, 130–137.
35 G. Zhang and C. Wu, *J. Am. Chem. Soc.*, 2001, **123**, 1376–1380.
36 J. Yin, X. Guan, D. Wang and S. Liu, *Langmuir*, 2009, **25**, 11367–11374.
37 C. D. Sorrell, M. C. Carter and M. J. Serpe, *Adv. Funct. Mater.*, 2011, **21**, 425–433.
38 O. Zavgorodnya and M. J. Serpe, *Colloid Polym. Sci.*, 2011, **289**, 591–602.
39 F. Zhang and C.-C. Wang, *Langmuir*, 2009, **25**, 8255–8262.
40 C. D. Sorrell and M. J. Serpe, *Anal. Bioanal. Chem.*, 2012, **402**, 2385–2393.
41 D. Wang, T. Liu, J. Yin and S. Liu, *Macromolecules*, 2011, **44**, 2282–2290.
42 V. Lapeyre, I. Gosse, S. Chevreux and V. Ravaine, *Biomacromolecules*, 2006, **7**, 3356–3363.
43 D. Schmaljohann, *Adv. Drug Delivery Rev.*, 2006, **58**, 1655–1670.
44 J. K. Oh, R. Drumright, D. J. Siegwart and K. Matyjaszewski, *Prog. Polym. Sci.*, 2008, **33**, 448–477.
45 T. Hoare, B. P. Timko, J. Santamaria, G. F. Goya, S. Irusta, S. Lau, C. F. Stefanescu, D. Lin, R. Langer and D. S. Kohane, *Nano Lett.*, 2011, **11**, 1395–1400.
46 M. C. Carter, C. D. Sorrell and M. J. Serpe, *J. Phys. Chem. B*, 2011, **115**, 14359–14368.
47 L. Hu and M. J. Serpe, *Polymers*, 2012, **4**, 134–149.
48 Y. Gao, W. Xu and M. J. Serpe, *J. Mater. Chem. C*, 2014, **2**, 5878–5884.
49 Y. Gao and M. J. Serpe, *ACS Appl. Mater. Interfaces*, 2014, **6**, 8461–8466.
50 Q. M. Zhang, A. Ahiabu, Y. Gao and M. J. Serpe, *J. Mater. Chem. C*, 2015, **3**, 495–498.
51 Q. M. Zhang, W. Xu and M. J. Serpe, *Angew. Chem.*, 2014, **126**, 4927–4931.
52 Y. Gao, A. Ahiabu and M. J. Serpe, *ACS Appl. Mater. Interfaces*, 2014, **6**, 13749–13756.
53 Y. Gao, G. P. Zago, Z. Jia and M. J. Serpe, *ACS Appl. Mater. Interfaces*, 2013, **5**, 9803–9808.
54 M. R. Islam, Y. Gao, X. Li and M. J. Serpe, *J. Mater. Chem. B*, 2014, **2**, 2444–2451.
55 C. D. Sorrell, M. C. Carter and M. J. Serpe, *ACS Appl. Mater. Interfaces*, 2011, **3**, 1140–1147.

